Synthesis of carbon nanofibers by catalytic pyrolysis of ethylene and methane on hydrides of intermetallic compounds of lanthanum with nickel

A. A. Volodin,[a] P. V. Fursikov,[a] Yu. A. Kasumov,[b] I. I. Khodos,[b] and B. P. Tarasov[a]★

[a]*Institute of Problems of Chemical Physics, Russian Academy of Sciences, 1 prosp. Akad. Semenova, 142432 Chernogolovka, Moscow Region, Russian Federation. Fax: +7 (496) 515 5420. E-mail: btarasov@icp.ac.ru*

[b]*Institute of Problems of Microelectronic Technology and Ultrahigh-Purity Materials, Russian Academy of Sciences, 6 ul. Institutskaya, 142432 Chernogolovka, Moscow Region, Russian Federation. Fax: +7 (496) 962 8047. E-mail: khodos@ipmt-hpm.ac.ru*

Carbon nanofibers were synthesized by the pyrolysis of ethylene and methane on hydrides of intermetallides $LaNi_nH_x$ (n = 2, 3, 5; x = 0.1—4). The influence of parameters of the synthesis (temperature and the ratio of gases in an Ar : H_2 : C_2H_4 (CH_4) mixture) on the structure of nanofibers thus formed was studied. Hydrides of nickel intermetallides are more efficient catalytic systems than metallic nickel.

Key words: pyrolysis, methane, ethylene, intermetallic compounds, carbon nanofibers, carbon nanotubes.

Nickel is widely used as a catalyst for the synthesis of carbon nanofibers (CNF) and nanotubes (CNT) by the pyrolytic decomposition of hydrocarbons.[1—3] Since the diameter of such carbon products depends substantially on the size of catalyst particles,[3—5] to decrease the thickness of CNF and CNT, the reaction zone should contain, in most cases, a catalyst in the form of nanosized metallic particles, which are not prone to agglomeration and sintering. For this purpose, it has previously[6,7] been proposed to use intermetallic compounds of nickel, in particular, $LaNi_5$ and $LaNi_2$. It is known that a certain chemical treatment of an intermetallide powder (etching in alkali) followed by the reduction of nickel oxide with hydrogen results in the formation of a metallic nickel phase on the intermetallide surface. This phase in the form of small particles further serves as a catalyst of hydrocarbon pyrolysis and CNF growth.

In the present work, the decomposition of hydrocarbons was carried out for the first time in the presence of intermetallides and their hydrides $LaNi_5H_x$ (x = 0—1), $LaNi_3H_x$ (x = 0—2), and $LaNi_2H_x$ (x = 0—4), which exist as highly dispersed powders obtained by the hydride dispersion of the starting alloy.[8] In this case, metallic nickel particles are formed directly during pyrolysis and, therefore, the starting intermetallide hydride is a precursor of the catalyst of formation and growth of CNF and CNT.[6,9]

The purpose of the present work is to find a relationship between the parameters of ethylene and methane pyrolysis (temperature and the composition of the gas phase), which are varied in a wide range, and the composition of carbon products and the structure of the carbon nanofibers and nanotubes thus formed.

Experimental

The catalytic synthesis of carbon nanomaterials was carried out in a cylindrical horizontal flow-type gas reactor (length 800 mm, diameter 40 mm) at temperatures in the reaction zone of 400—900 °C and a pressure of 0.1 MPa. Powders of $LaNi_5H_x$, $LaNi_3H_x$, and $LaNi_2H_x$ with a particle size of 1—10 μm were prepared by tenfold repetition of hydrogenation—dehydrogenation cycles of an alloy of the corresponding intermetallide.[8] The hydrogen content of hydrides depends on the dehydrogenation temperature and changes from ~0.05 to 4. In all experiments, $LaNi_nH_x$ powders (n = 2, 3, 5) with a weight of 0.1 g were poured as thin layers (~0.3 mm) on the bottom of a quartz boat, which was placed in the center of the reactor. Mixtures of C_2H_4, H_2, and Ar were used in different ratios. In all experiments, the flow rate of ethylene was constant, being 40 $cm^3\ min^{-1}$, as well as the overall flow rate of the mixture (140 $cm^3\ min^{-1}$). The composition of the gas phase was varied by changing the flow rate of H_2 and Ar. The procedure of synthesis was described in detail earlier.[9] Experiments on nickel and iron powders similar to the intermetallides in crystallite size (1—10 nm) were carried out under the same conditions for comparison. In several experiments at T > 750 °C, methane was used instead of ethylene. When the weight of carbon pyrolysis products was determined, only the soot formed within 1 h on the surface of the intermetallide hydride powder was taken into account. Such an amount of the soot that deposited on 1 g of the initial powder was accepted to be the yield of the soot.

Published in Russian in *Izvestiya Akademii Nauk. Seriya Khimicheskaya,* No. 10, pp. 2210—2214, October, 2005.

1066-5285/05/5410-2281

Products of the synthesis were studied by transmission electron microscopy (TEM) on EMV-100B and JEOL JEM-2000FXII electron microscopes, oxidative thermogravimetry (OTG) on a Q-1000 derivatograph, X-ray phase diffraction analysis (XRD) on a DRON-1 setup (Cr-Kα radiation), and electron probe X-ray microanalysis (EPXMA) on a JEOL JEM-2000FXII electron microscope equipped with an attachment for measurements of the characteristic X-ray radiation with energy dispersion. To prepare a sample for studies by the TEM and EPXMA methods, the sample was ultrasonically suspended in acetone, and the suspension was deposited onto a copper network.

Results and Discussion

It has previously[9] been shown that the weight of the soot formed upon pyrolysis increases linearly as the time of the process increases (to at least 4 h) and with an increase in the weight of the starting intermetallide hydride (up to 0.4 g). In the temperature and partial hydrogen pressure ranges used in the work, the reaction of ethylene decomposition is thermodynamically favorable, and the growth of carbon nanostructures (CNS) is determined by the kinetic regularities.

Elemental analysis of the samples obtained by ethylene pyrolysis at different temperatures showed[9] that the hydrogen content in the soot did not exceed 1.5%, and the Ni : La ratio in the soot is similar to the ratio in the starting intermetallide.

For ethylene pyrolysis, a noticeable formation of soot on the catalyst surface begins at 400 °C, and the onset temperature is 700 °C in the case of methane. Above 750 °C, ethylene is thermally decomposed predominantly in the gas phase. The temperature in the reactor and the gas mixture composition affect substantially the weight of the soot that formed. We failed to reveal any distinct dependence of the soot weight on the composition of the intermetallide used. As a whole, the character of the dependence of the soot yield on the temperature and composition of the gas mixture is similar for all intermetallides under study. For instance, the maximum yield of the carbon products of ethylene pyrolysis in the absence of hydrogen is observed at 500—550 °C (Table 1, Fig. 1). When $LaNi_5H_x$ is used, the soot yield is much higher, as a rule, than that in the case of $LaNi_3H_x$ and $LaNi_2H_x$.

The growth of CNF and CNT depends on the rate of hydrocarbon decomposition on the surface of a metallic particle or in the bulk of this particle and on the rate of carbon deposition. The total yield of the pyrolysis products decreases with the temperature increase, because the rate of carbon supply from the gas phase into the bulk of a metallic catalyst particle exceeds the rates of diffusion and carbon deposition, which results in coking of catalytic particles and in terminating the CNS growth. However, according to the OTG data, the relative fraction of graphitized components, including CNF and CNT, increases with an increase in the temperature of the process (Fig. 2). The ratio of the weight loss of the sample at $T > 550$ °C to the weight loss of the sample in the whole interval of temperature rise (100—950 °C) was accepted as this fraction. This choice of the temperature for the quantitative estimation of the content of nanotubes and graphitized nanofibers in the soot is confirmed by literature data.[10,11]

Table 1. Weight of the soot formed at different temperatures of C_2H_4 pyrolysis and different Ar : H_2 ratios*

Flow rate /mL min^{-1}		Soot weight /g (g $LaNi_nH_x$)$^{-1}$			n**
Ar	H_2	500 °C	600 °C	700 °C	
100	0	0.78	0.68	0.37	2
		14.14	0.69	0.53	3
		13.74	3.86	1.00	5
75	25	16.40	2.10	1.85	2
		14.57	3.09	0.95	3
		16.41	3.47	4.77	5
50	50	16.64	7.37	2.03	2
		15.78	6.11	2.19	3
		17.47	12.88	4.91	5
25	75	16.59	6.92	2.57	2
		17.20	12.89	3.63	3
		19.48	16.59	5.07	5
0	100	14.86	17.00	3.82	2
		13.37	14.48	3.04	3
		15.62	17.15	5.11	5

* The flow rate of ethylene is 40 mL min^{-1}.
** In the starting $LaNi_nH_x$ powder.

The yield of the pyrolysis products increases upon the addition of hydrogen to the gas mixture (Table 2). In addition, an increase in the hydrogen content slightly shifts the maximum on the temperature plot of the soot

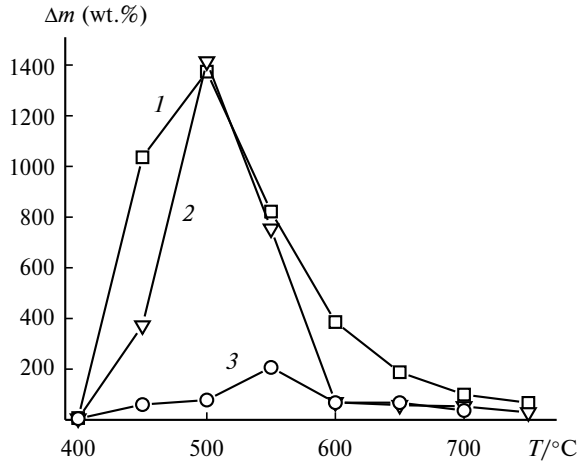

Fig. 1. Increase in the soot weight (Δm) *vs.* temperature of ethylene pyrolysis in the absence of hydrogen in a gas mixture on $LaNi_5H_x$ (*1*), $LaNi_3H_x$ (*2*), and $LaNi_2H_x$ (*3*).

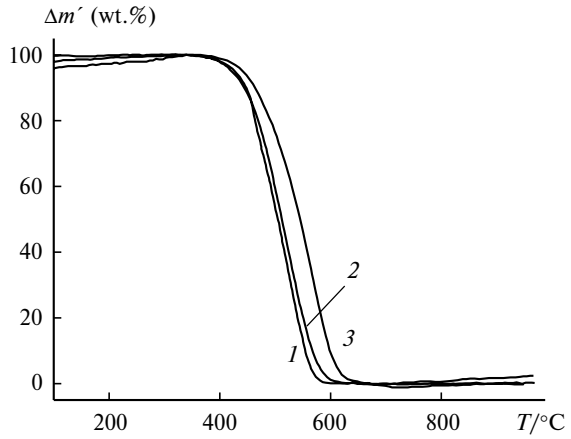

Fig. 2. Thermograms of oxidation of the samples obtained by ethylene pyrolysis at 500 (*1*), 600 (*2*), and 700 °C (*3*) in the presence of $LaNi_5H_x$. The heating rate in an air flow is 10 °C min^{-1}; $\Delta m'$ is the weight loss of the sample.

yield toward higher temperatures (see Table 1). In the studied range of variation of the composition of the gas mixture that is supplied to the reactor, the total soot yield is especially high at the ratio of components $C_2H_4 : H_2 : Ar = 1.6 : 3 : 1$. An increase in the hydrogen content in the mixture for each temperature also favors a decrease in the amount of amorphous pyrocarbon in the products and an increase in the fraction of products with a more graphitized structure (see Table 2).

To explain the influence of hydrogen, it can be postulated that hydrogen interacts with soot precursors, which are the fragments C_xH_y ($x = 1, 2$; $y = 0—3$) adsorbed on the surface of nickel crystallites, and returns hydrogenated species into the gas phase.[12] Hydrogen thus prevents coking of the working surface of the catalyst particles and decreases the relative fraction of the amorphous component in carbon products of the synthesis. The further increase in the hydrogen content results in the overall decrease in the soot yield.

The character found for the effect of the pyrolysis temperature and composition of the gas mixture supplied into the reactor on the process of CNS formation agrees, as a whole, with the mechanism of CNS growth.[2] It can

Table 2. Relative weight fraction of the well graphitized CNS in the products of ethylene pyrolysis

Temperature of synthesis/°C	Weight fraction of CNS (wt.%) at different H_2 contents in mixture (vol.%)		
	0	35	70
500	13	46	57
600	20	41	55
700	45	52	56

Note. The catalyst precursor was $LaNi_5H_x$.

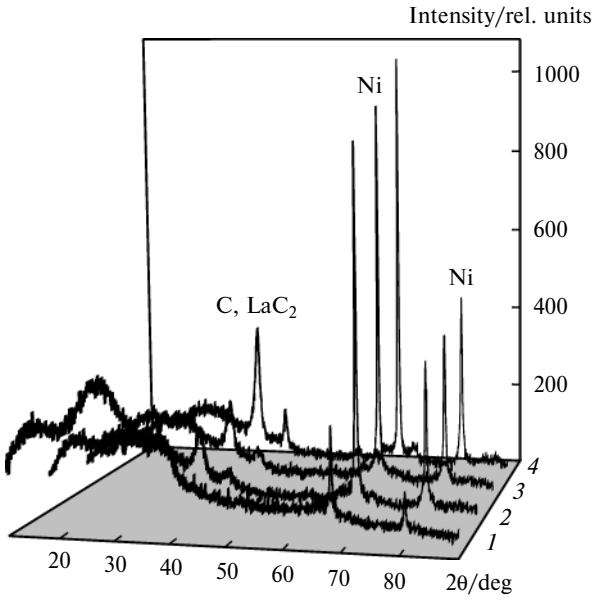

Fig. 3. Diffraction patterns of the pyrolysis products prepared at 450 (*1*), 500 (*2*), 650 (*3*), and 750 °C (*4*).

be assumed that H atoms are successively abstracted from a chemisorbed C_2H_4 (CH_4) particle on one of the faces of Ni crystallites. Then the C atoms are "dissolved" in the metallic particle bulk and diffuse to the opposite surface on which carbon is deposited and the CNS grow. To ensure an efficient growth of the CNS, the rate of carbon deposition should exceed the rate of carbon supply from the gas phase. Otherwise, the catalyst surface is coked.

The X-ray diffraction data for the products of the synthesis indicate that they contain phases of metallic Ni ($d = 2.04$ and 1.76 Å), LaC_2 ($d = 3.40$ and 2.12 Å), and graphite ($d = 3.36$ Å) (Fig. 3). These data suggest that the interaction with hydrocarbon on the surface of the hydrides of intermetallic compounds results in the formation of lanthanum carbide and nickel particles, and the latter function as the catalysts of CNS growth. The X-ray diffraction data show that the specific fraction of crystalline nickel and graphitized carbon increases in the sample with an increase in the pyrolysis temperature (see Fig. 3). Perhaps, lanthanum carbide plays a role of a unique carrier preventing the agglomeration of fine nickel particles.

As shown by special independent experiments, the growth of CNF is rather impeded if nickel or iron powders with the same dispersity are taken instead of the intermetallide hydrides. This is illustrated by the microphotographs in Fig. 4, which shows the presence of coked catalytic particles and individual fibers.

According to the TEM data, the nanofibers obtained by ethylene pyrolysis on $LaNi_5H_x$ at 500—750 °C, in the most cases, have a diameter of 10—30 nm. The fibers most frequently have an internal cavity (Fig. 5). Bridges are seen in some places of the cavities. The most thin and straight fibers have the structure of multiwall nanotubes

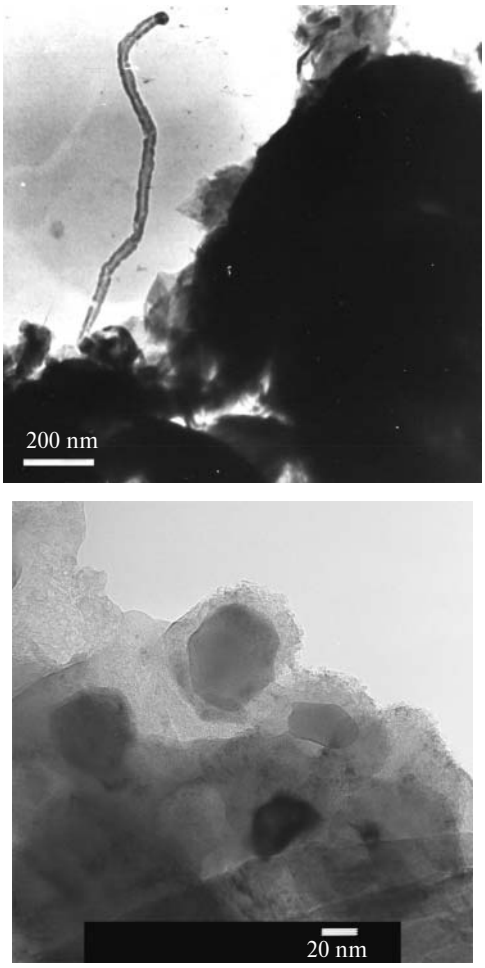

Fig. 4. Microphotographs of the samples obtained by ethylene pyrolysis in the presence of highly dispersed powders of Ni (*a*) and Fe (*b*) (carbon deposits covering the metallic particles are seen).

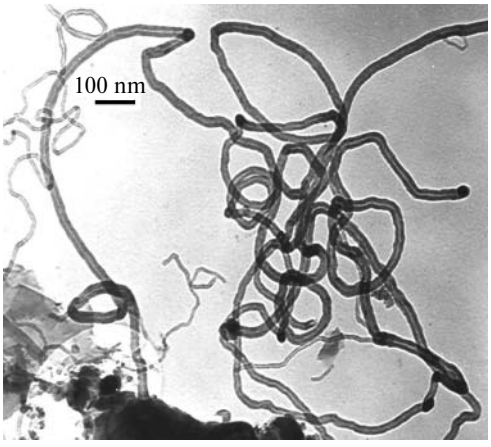

Fig. 5. Microphotograph of nanofibers in the sample obtained by ethylene pyrolysis on $LaNi_5H_x$ at 700 °C.

with walls representing coaxially inserted graphene cylindrical layers.

Metallic nickel particles are often observed on the ends of the fibers, which is confirmed by the EPXMA data (Fig. 6, *a*, inset). The spectra distinctly show peaks designating the presence of nickel in the region of analysis. The size of the nickel particles approximately coincide with the CNF diameter. This additionally indicates that the fiber grows on these particles. However, the peak of lanthanum in the EPXMA spectrum obtained "in the point" is absent (see Fig. 6, *a*). This indicates that the nickel particles are separated from lanthanum carbide particles upon the decomposition of the starting intermetallide and the CNS growth on the nickel particles. Nevertheless, the peak of lanthanum is present in the

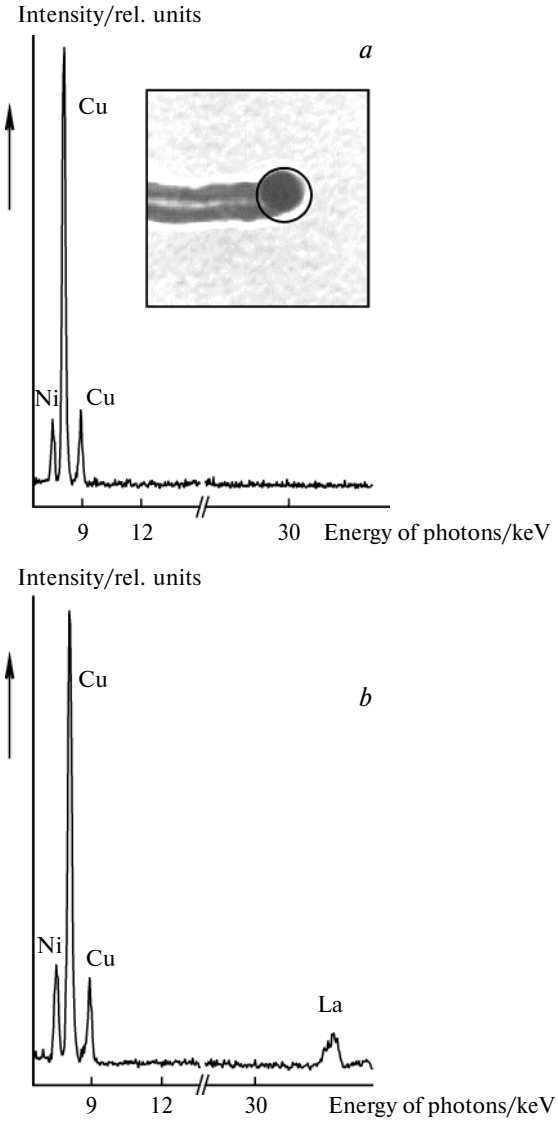

Fig. 6. EPXMA spectra of the sample obtained by ethylene pyrolysis on $LaNi_5H_x$ at 750 °C "in the point" (*a*) and for scanning over the surface (*b*). The beam diameter is ~20 nm. The site where EPXMA is performed (a metallic Ni particle formed at the fiber end) is shown in inset.

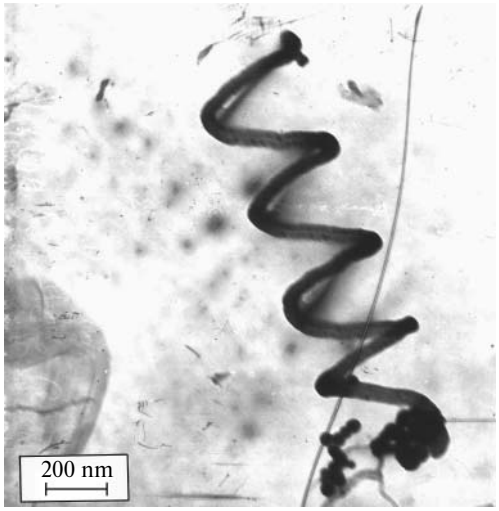

Fig. 7. Microphotograph of the spiral nanofiber in the sample obtained by ethylene pyrolysis on $LaNi_5H_x$ at 750 °C.

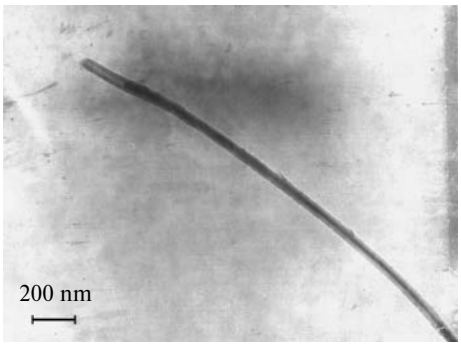

Fig. 8. Microphotograph of the nanofiber as a wire in the sample obtained by methane pyrolysis on $LaNi_5H_x$ at 800 °C.

EPXMA spectrum detected in a region with the large surface area (see Fig. 6, *b*). Its intensity is relatively low, because heavy lanthanum carbide is difficult to get onto the copper network during sample placing on this network.

At temperatures above 750 °C, spiral CNF appear in the soot samples (Fig. 7). The mechanism proposed for the growth of a spiral fiber[13] is concerned with the difference of the rates of carbon deposition on different faces of a metallic particle. Anisotropy of a catalyst particle also results in the situation when the carbon diffusion rate depends on the chosen direction. When assuming the Arrhenius dependence of the diffusion rate constant on the temperature, then the temperature rise should increase the difference in the rates, which favors the formation of fibers twisted in a spiral.

In some cases, the internal cavity of the fibers is partially filled with a metal, presumably, nickel. Such a nanowire with a diameter of ~20—40 nm obtained by the pyrolysis of CH_4 but at a higher temperature (800 °C) is presented in Fig. 8.

Intermetallide hydrides $LaNi_5H_x$, $LaNi_3H_x$, and $LaNi_2H_x$ are efficient precursors of the catalysts for the synthesis of carbon nanostructures, *viz.*, nanofibers. The interaction with hydrocarbons from the gas phase on the intermetallide surface produces LaC_2 and Ni particles (with a size of 10—50 nm), and the latter serve as catalysts of the CNS growth. Nanofibers formed on these particles have approximately the same size in the cross section. The maximum yield of the CNF for C_2H_4 pyrolysis using $LaNi_5H_x$, $LaNi_3H_x$, or $LaNi_2H_x$ as the catalyst precursors is observed at 500—550 °C. The decomposition of CH_4 on these powders at a higher temperature produces nanotubes filled with nickel having an average diameter of ~20 nm along with the nanofibers. The nanofibers with the graphitized structure are formed with an increase in the temperature of synthesis and the hydrogen content in the gas mixture.

This work was financially supported by the Russian Foundation for Basic Research (Project No. 04-03-97255), the Council on Grants of the President of the Russian Federation (Program of State Support for Young Russian Scientists, Grant MK-1083.2004.3), the International Scientific Technical Center (Grant 2760), and the Division of Chemistry and Materials Science of the Russian Academy of Sciences (Theme No. 8).

References

1. E. G. Rakov, *Usp. Khim.*, 2000, **69**, 41 [*Russ. Chem. Rev.*, 2000, **69** (Engl. Transl.)].
2. V. V. Chesnokov and R. A. Buyanov, *Usp. Khim.*, 2000, **69**, 675 [*Russ. Chem. Rev.*, 2000, **69** (Engl. Transl.)].
3. V. I. Trefilov, D. V. Shchur, B. P. Tarasov, Yu. M. Shul´ga, A. V. Chernogorenko, A. V. Pishuk, and S. Yu. Zaginaichenko, *Fullereny — osnova materialov budushchego* [*Fullerenes As the Basis for Materials of the Future*], ADEF, Kiev, 2001, 148 pp. (in Russian).
4. N. M. Rodriguez, *J. Mat. Res.*, 1993, **8**, 3233.
5. H. Dai, A. G. Rinzler, and P. Nikolaev, *Chem. Phys. Lett.*, 1996, **260**, 471.
6. X. P. Gao, X. Qin, and F. Wu, *Chem. Phys. Lett.*, 2000, **327**, 271.
7. X. P. Gao, Y. Zhang, and X. Chen, *Carbon*, 2004, **42**, 47.
8. B. P. Tarasov, *Hydrogen Materials Science and Chemistry of Metal Hydrides. NATO Science Series. II*, 2002, **71**, 275.
9. A. A. Volodin, P. V. Fursikov, and B. P. Tarasov, *Al´ternativnaya energetika i ekologiya* [*Alternative Energetics and Ecology*], 2002, **6**, 34 (in Russian).
10. B. C. Liu, S. H. Tang, and Z. L. Yu, *Chem. Phys. Lett.*, 2002, **357**, 297.
11. P. V. Fursikov and B. P. Tarasov, *Al´ternativnaya energetika i ekologiya* [*Alternative Energetics and Ecology*], 2004, **10**, 24 (in Russian).
12. P. Chen, H.-B. Zhang, and G.-D. Lin, *Carbon*, 1997, **35**, 1495.
13. Y. Wen and Z. Shen, *Carbon*, 2001, **39**, 2369.

Received July 27, 2005